Pergamon

Cement and Concrete Research 32 (2002) 893–901

CEMENT AND CONCRETE RESEARCH

Chloride ingress and steel corrosion in cement mortars incorporating low-quality fly ashes

Kwasi Osafo Ampadu, Kazuyuki Torii*

Department of Civil Engineering, Kanazawa University, 20-40-20 Kodatsuno, Kanazawa 920-8667, Japan

Received 6 March 2001; accepted 16 December 2001

Abstract

In this study, the microstructure and hydration characteristics of ecocement and normal Portland cement mortars blended with low-quality fly ashes were investigated. In addition, the corrosive behaviours of steel bars embedded in the mortars were studied. Several tests including scanning electron microscopy (SEM), X-ray diffraction (XRD) analysis and differential scanning calorimetry (DSC) were used for the characterization of the mortars. Electrochemical measurement such as linear polarization resistance and AC impedance spectroscopy were also used to monitor the corrosive behaviours of the embedded steel bars in the mortars. The chloride ingress into the mortars was also studied. The results of the various tests are discussed.

Keywords: Fly ash; Microstructure; Chloride ingress; AC impedance; Corrosive behaviour; Electrochemical measurements

1. Introduction

It is well known that blending cement with fly ash or other supplementary cementing materials like slag and silica fume improves the rheological properties of the fresh concrete and the engineering properties of the hardened concrete. In particular, both the improvement in the consistency and bleeding of the fresh concrete and the improvement in strength and durability of the hardened concrete have been reported [1,2]. These improvements are generally attributed to both the physical and chemical effects. The physical process is due to the fineness of the particles of the supplementary cementing materials that are much smaller than that of the cement, thereby providing densely packed particles between the fine aggregates and the cement grains, and hence, a reduction in porosity. The chemical process is due to the activation of the noncrystalline silica, the major constituent of fly ash, by the calcium hydroxide produced from the hydrating cement to form secondary calcium silicate hydrate that also fills the pore spaces and further reduces the porosity. The reactivity of fly ash has been found to depend on the mineral substitution in the glassy silica structure. Fly ashes containing high amounts of calcium oxide have both cementing and pozzolanic activity while those containing mainly aluminium oxide and iron oxide as the major mineral substitution in the structure of the silica glass only has pozzolanic activity. According to the ASTM classification, fly ashes are broadly classified into two broad categories, Class F and Class C, based on their chemical compositions. The ASTM C 618 further sets limits for the particle size and the loss on ignition, as these are known to affect the properties of concrete produced with fly ash-blended cement. On the other hand, the Japanese Industrial Standard (JIS A6201-1999) has classified the fly ash into four classes. This is because recently, many electric power companies have emerged, using coals from various sources of overseas supply in the power plants. As a result, various grades of fly ashes have emerged, prompting the Japanese industrial standard (JIS A6201-1999) to broaden their classification for fly ash in concrete. In some cases, most of the fly ashes produced are low in quality, which are used only for landfills and for land reclamation purposes near the power plants. There is, however, an environmental concern, and also, a scarcity of dumping sites, making the search for better use for them imperative. This study therefore aims at investigating the beneficial or adverse effects when these low-quality fly ashes are blended with cements. In particular, the study seeks to investigate bene-

* Corresponding author. Tel.: +81-76-234-4620; fax: +81-76-234-4632.
E-mail address: torii@t.kanazawa-u.ac.jp (K. Torii).

0008-8846/02/$ – see front matter
PII: S0008-8846(02)00721-4

ficial or adverse properties regarding compressive strength, chloride binding ability and protection of embedded steel against the aggressive saline environment [3]. X-ray diffraction (XRD), differential scanning calorimetry (DSC), and scanning electron microscopy (SEM) were used to characterize the microstructure, and also to determine the hydration products of the cement mortars with and without fly ashes. In addition, electrochemical methods such as linear polarization resistance and AC impedance measurements were used to monitor the corrosive behaviour of steel bars embedded in the mortars.

2. Experimental

2.1. Materials

The materials used for the experiment are the two types of low-quality fly ash, normal Portland cement and ecocement, which is a new type of hydraulic cement produced using incinerator ash as part of the raw materials [4,5]. Table 1 shows the chemical compositions of the cements. The essential difference between ecocement and NPC is that the former contains calcium chloro-aluminate ($C_{11}A_7CaCl_2$) in mineral composition, eliminating C_3A, which contributes to rapid hardening. Table 2 shows a translated version of the revised JIS classification for fly ashes. Two types of fly ash with physical and chemical properties shown in Table 3 were used for this study. Comparison of Table 3 with the JIS standards indicates that Fly ash A is classified as Type IV while Fly ash B lies outside any of the four classes in Table 2. It is also seen that the ignition losses for Fly ash B is very high, and that its Blaine fineness is higher than that of fly ash Class I in the JIS classification. This may be due to the large content of residual carbon. Also, the particles of Fly ash A are very coarse, with a percentage retained on the 45-μm sieve size being more than 34%, the limiting value according to ASTM C 618. Both Fly ashes A and B have high silica content. Fig. 1 shows the SEM micrographs of Fly ashes A and B. It is seen that Fly ash A contains a larger percentage of spherical particles than Fly ash B, which rather contains a lot of irregularly shaped porous particles probably due to its high content of residual carbon.

2.2. Mortar mixture proportions

Each of the two types of fly ash was blended with the NPC and ecocement to prepare mortar specimens at a water to binder ratio of 0.55. Fly ash replacement percentages of 20% and 40% were used in the mortar mixture. In addition, control specimens were prepared (i.e., without fly ash) for each type of cement. Table 4 shows the mixture proportions of the mortars. Two sets of cylindrical mortar specimens of 50 mm in diameter and 100 mm high were cast. After demoulding, the mortar specimens were moist-cured for 7 days. The sides and top surface of one set of the specimens, to be used for the determination of chloride ion diffusion coefficient, were coated with the epoxy resin leaving the bottom surface uncoated in order to simulate a one-dimensional diffusion. The other set, which was to be used for the microstructure characterization, was cured in a saturated calcium hydroxide solution. In addition, two sets of mortar specimens with dimensions 170 × 100 × 60 mm with a 10-mm diameter × 160-mm length mild steel and stainless steel bars embedded at a cover depth of 10 mm were also prepared for corrosion monitoring. External stainless steel plugs were connected to one end of the steel bars to serve as contact points for electrical connection. Fig. 2 shows a picture of a typical specimen used for the corrosion monitoring. One set was moist-cured for 7 days and the other set cured for 28 days. After curing, their exposed surfaces were coated with an epoxy resin leaving only the top surface uncoated, and were placed in an environmental chamber together with the epoxy-coated cylindrical specimens. While in the environmental chamber, the specimens were sprayed with a 5% NaCl solution for 8 h followed by a 16-h dry period in an alternate wet and dry cycle. A temperature and relative humidity of 40 °C and of 100%, respectively, were maintained during the wet cycle and were changed to 20 °C and 50% during the dry cycle.

Table 1
Chemical compositions of the binders used for the study (%)

Cement type	Ignition loss	SiO_2	Al_2O_3	Fe_2O_3	CaO	MgO	SO_3	Na_2O	K_2O	Cl
NPC	1.6	21.7	5.3	2.9	63.7	1.2	2.1	0.3	0.5	0.0
ECO	0.5	14.9	10.5	2.5	56.7	1.7	9.2	0.8	0.01	0.8

Table 2
Classification of fly ash according to JIS A6201-1999

	Fly ash Type I	Fly ash Type II	Fly ash Type III	Fly ash Type IV
Silica content (%)	>45.0			
Moisture content (%)	<1.0			
Ignition loss (%)	<3	<5	<8	<5
Specific gravity (g/cm^3)	>1.95			
Fineness				
Retained on 45 μm sieve (%)	<10	<40	<40	<70
Blaine fineness (cm^2/g)	>5000	>2500	>2500	>1500
Flow value (%)	>105	>95	>85	>75
Pozzolanic activity index (%)				
28 days curing	>90	>80	>80	>60
91 days curing	>100	>90	>90	>70

2.3. Experimental measurements

2.3.1. Microstructure and hydration products characterization

After curing times of 7, 28, and 91 days immersed in the saturated calcium hydroxide solution, powder XRD

Table 3
Physical properties of fly ash used for the study

	Type (JIS A6201)	Ignition loss (%)	MB[a] (mg/g)	Blaine fineness (cm^2/g)	Retained on 45 μm sieve (%)	SiO_2 (%)	Specific gravity (g/cm^3)	Moisture content (%)
Fly ash A	IV	4.18	1.13	4060	40.9	48.7	2.06	0.15
Fly ash B	No class	14.3	1.96	5400	23.3	47.4	2.02	0.15

[a] Methylene blue absorption test value additional test for residual carbon (Japan Cement Association Standard, JCAS I-61).

analysis and DSC were conducted on samples taken from the cylindrical mortar specimens. Both electrical resistivity and compressive strength were also conducted to monitor the rates of hydration and strength development of the mortar specimens.

2.3.2. Electrochemical measurements

The linear polarization resistance and the AC impedance measurements were conducted biweekly to monitor the corrosive behaviours of the embedded steel bars in the mortars. The measurements were repeated until some of the specimens showed a severe cracking resulting from the corrosion of embedded steel bars.

After the corrosion-monitoring test, the mortar specimens were split open after the end of the experiment, and the steel bars were carefully removed from the embedded mortars. Their corroded areas were measured. The rust on the steel bars was then removed by immersion in 10% di-ammonium hydrogen citrate solution at a temperature of 50 °C for 24 h. After removal, they were cleaned of all rust and then weighed to determine their weight loss resulting from the corrosion.

2.3.3. Chloride concentration profiles

At the end of the exposure period, the cylindrical mortar specimens that were placed in the environmental chamber were removed. For each specimen, five discs of thickness 10 mm each were sliced, starting from the top surface. These were then ground into fine powder passing the 150-μm sieve size. The total chloride contents were then measured in accordance to the JCI-SC 5 standard. In this measurement procedure, a 2-M HNO_3 solution was added to the powder, and the mixture was titrated with 0.005 M $AgNO_3$ solution to determine the total chloride content of the mortar powder. The results were then used to plot a graph of the chloride content versus depth measured from the surface of the cylindrical specimen.

3. Results and discussion

3.1. Compressive strength and electrical resistivity

Fig. 3 shows the variation of compressive strength with curing time of the mortar specimens. The graph shows that the rate of strength development of the cement–fly ash mortars is slower in comparison to that of the control specimens. It is seen that in both NPC and ecocement, the compressive strength of the mortar specimens blended with 20% of Fly ash A is quite close to that of the control specimen at the latter ages of hydration. On the other hand, 20% cement replacement by Fly ash B results in about 10% and 16% reduction in compressive strength in NPC and ecocement, respectively, as at 24 weeks of hydration, while 40% cement replacement by both Fly ashes A and B results in about 25% reduction in compressive strength in both cements. Also, the compressive strengths of the ecocement mortars are not significantly different from that of corres-

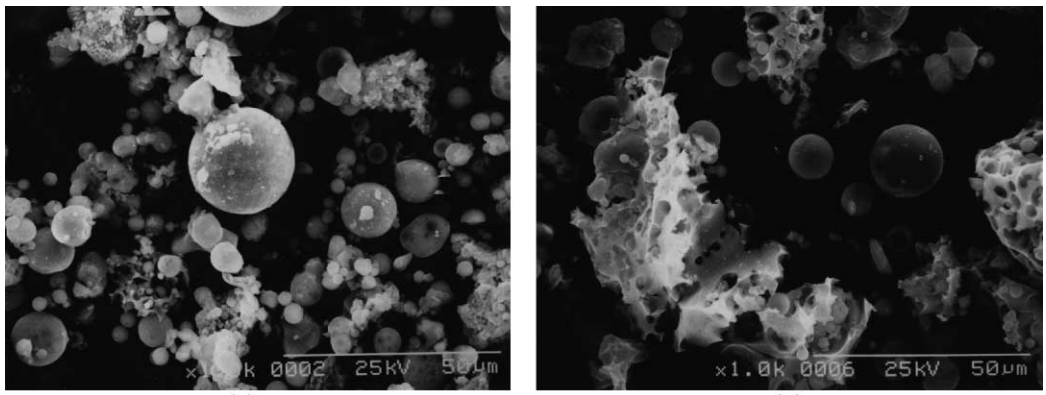

Fig. 1. SEM micrographs of Fly ash A (left) and Fly ash B (right).

Table 4
Mixture proportions of mortar specimens (kg/m^3)

Specimen name[a]	w/c	Water	Cement	Fly ash	Sand	Retarder[b]	Chloride content
Control	0.55	336	611	0	1222	–	–
O7FA20, O28FA20			489	122			
O7FA40, O28FA40			367	244			
O7FB40, O28FB40			367	244			
Control	0.55	336	611	0	1222	2.44	4.89
E7FA20, E28FA20			489	122		1.95	3.91
E7FA40, E28FA40			367	244		1.46	3.91
E7FB40, E28FB40			367	244		1.46	2.94

[a] E: Ecocement, O: NPC, FA: Fly ash A, FB: Fly ash B.
[b] Citric acid is used for rapid-hardening type ecocement.

ponding NPC specimens. Thus, with respect to compressive strength, blending NPC or ecocement with 20% of Fly ash A or B could be accommodated in applications requiring the concrete of normal strength.

Fig. 4 shows the graph of electrical resistivity with curing time of the mortar specimens. It is seen that the electrical resistivity of the fly ash-blended specimens of NPC increases at a faster rate than that of the corresponding ecocement specimens. Since electrical resistivity depends on both the porosity and ionic concentration in the pore solutions of mortars, its rate of change is an indirect measure of the rate of hydration. Also, since the rate of change of electrical resistivity of the control specimens of both cements is very low in comparison to that of the fly ash-blended specimens, it could be inferred that it is the pozzolanic reaction of the fly ash that results in a high rate of change of the electrical resistivity. Thus, comparison of the graphs of ecocement and NPC indicates that pozzolanic reactivity in ecocement–fly ash is less than that of NPC–fly ash. The graphs also show that pozzolanic reaction is not completed at 24 weeks of hydration.

3.2. Chloride ingress

Figs. 5 and 6 show the chloride concentration profiles of the mortar specimens at 40 weeks of exposure to the severe saline environment. It is seen that in both sets of specimens moist-cured for 7 and 28 days before exposure to the saline environment, the addition of both types of fly ash to the cements results in a significant reduction in chloride ingress beyond the depth of 20 mm compared with the mortars without fly ash. Also, in both cements, the chloride profiles of the Fly ash B-blended mortars are lower in comparison to that of corresponding Fly ash A-blended specimens, while in both fly ashes, 40% cement replacement results in the lowest chloride ingress at deeper depths.

3.3. Corrosion current

Figs. 7 and 8 show the graphs of the corrosion current versus exposure time of the steel bars embedded in the 7- and 28-day cured mortars of both NPC and ecocement. A sudden transition in the corrosion current, from low

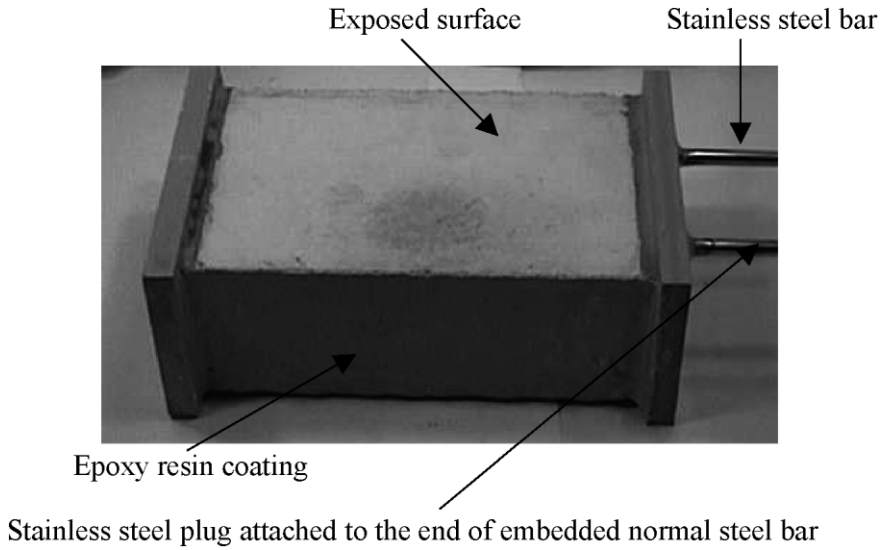

Fig. 2. Specimen for monitoring corrosion of embedded steel bars (cover thickness: 10 mm).

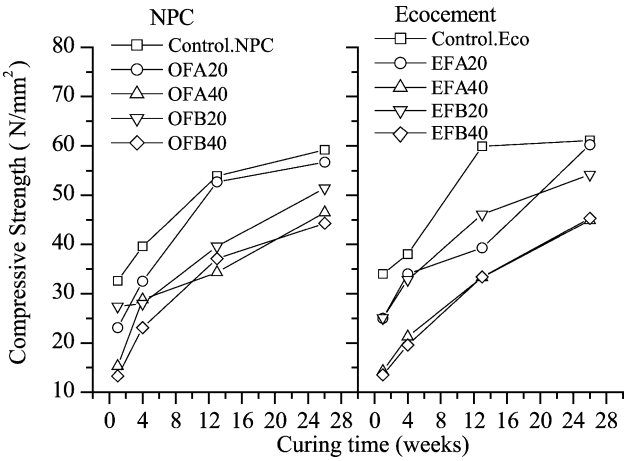

Fig. 3. Compressive strength versus curing time of mortar specimens.

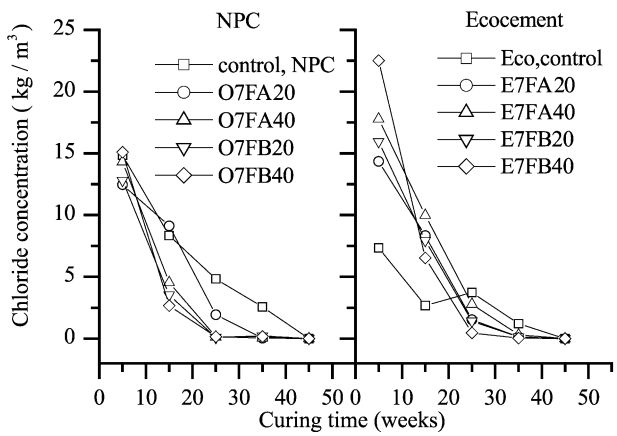

Fig. 5. Chloride concentration profiles for the mortar specimens moist-cured for 7 days before placing in the environmental chamber.

values to values above 0.1 μA/cm^2, is an indication of corrosion initiation [6]. It is seen that in the case of NPC specimens, there was a significant extension in the time to corrosion initiation of the steel bar embedded in the mortar with 40% replacement by Fly ash A when the initial curing period before placing in the environmental chamber was changed from 7 to 28 days, while in the case of Fly ash B there was no significant extension in the time to corrosion initiation. Also, in the case of the control specimen precured for 7 days before placing in the environmental chamber, corrosion initiation of the embedded steel bar occurred at 18 weeks of exposure, while there was no corrosion at 40 weeks of exposure in the case of the control specimen precured for 28 days. In the ecocement specimens, corrosion initiation occurred within the first 5 weeks of exposure to the saline environment in the steel bars embedded in the fly ash-blended mortars of both the specimens precured for 7 and 28 days before placing in the environmental chamber. On the other hand, in the case of the control specimen precured for 7 days before placing in the environmental chamber, corrosion initiation of the embedded steel bar occurred at 5 weeks of exposure to the severe saline environment, while there was no corrosion at 40 weeks of exposure in the case of the control specimen precured for 28 days. The figures seem to suggest that the addition of the fly ash to both cements rather results in a negative effect with respect to corrosion of embedded steel bars. However, as discussed above, the addition of the fly ash to the cements actually results in a significant reduction of chlorides at deeper cover depths. The cover depth of 10 mm used in this preliminary study is, however, too small for expecting the beneficial effect of the fly ash, with respect to the corrosive behaviours of the embedded steel bars to be manifested. The chloride profiles in Figs. 5 and 6 show that an increase in the cover thickness from 10 to 20 mm or more would, to a large extent, reduce the concentration of chloride ions on the surface of the steel, and hence, result in very low corrosion rates in the embedded steel bars. It should, however, be mentioned that similar studies using specimens with a cover depth of 20 mm is

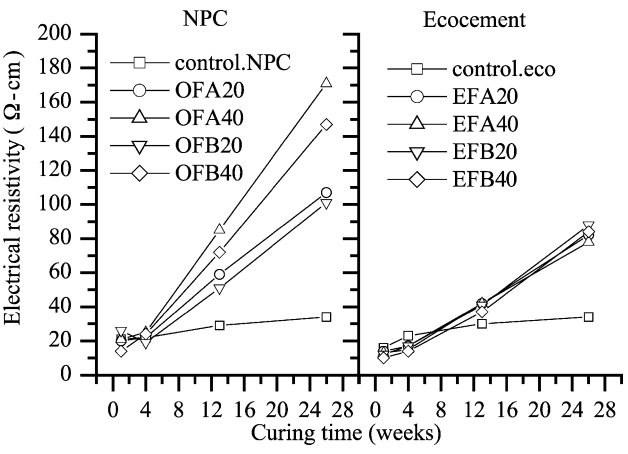

Fig. 4. Electrical resistivity versus curing time of mortar specimens.

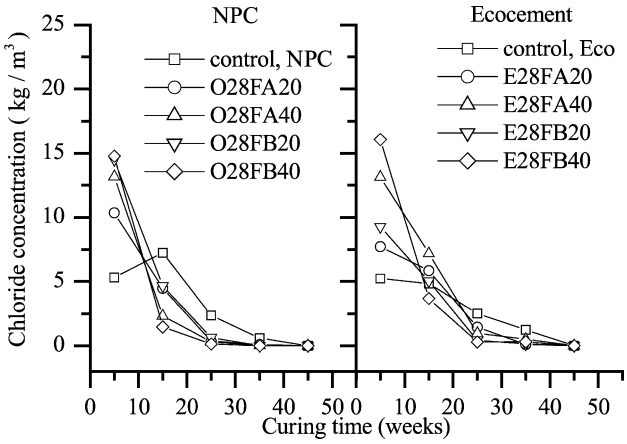

Fig. 6. Chloride concentration profiles for the mortar specimens moist-cured for 28 days before placing in the environmental chamber.

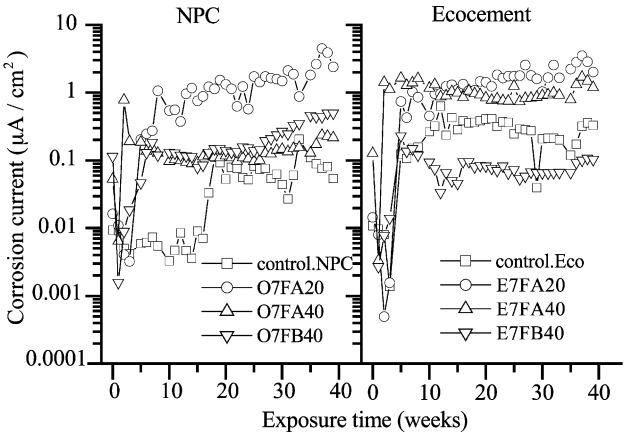

Fig. 7. Corrosion current versus curing time for specimens moist-cured for 7 days before placing in the environmental chamber.

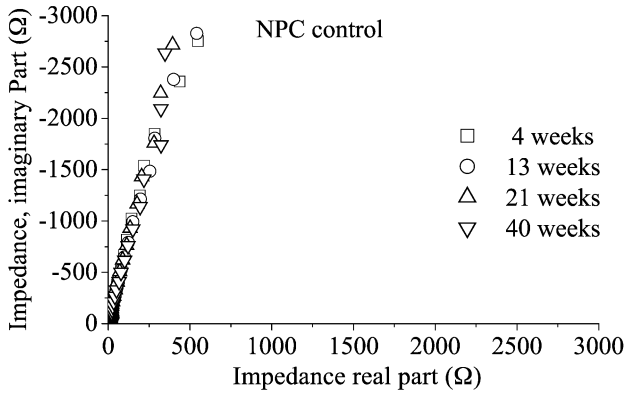

Fig. 9. Impedance plane plots for the NPC control specimen moist-cured for 28 days before placing in environmental chamber.

currently under study and the current results indicate that corrosion initiation has not yet begun at 41 weeks of exposure to the same environment. The final result would also be published.

3.4. AC impedance

Figs. 9 and 10 show the impedance plane plots of the control specimen of NPC and that blended with 20% fly ash at various times of exposure to the saline environment. In AC impedance measurements, the diameter of the arc obtained in the impedance plane plot is equivalent to the polarization resistance. It is seen that in the case of the fly ash-blended specimen, the diameter of the arc decreases with exposure time, indicating a gradual increase in the corrosion rate of the embedded steel bar. On the other hand, there is almost no change in the impedance plane plot of the control specimen with exposure time, indicating that the embedded steel bar remained in the passive state at 40 weeks of exposure. This result is in agreement to that of the linear polarization resistance measurement.

3.5. Hydration product characteristics

Figs. 11 and 12 show typical DSC curves for the NPC and ecocement mortar specimens taken from around the steel bars. The figure shows that the calcium hydroxide content in the mortars of both cements, which is equivalent to the area under the endothermic peak around 460 °C, decreases with fly ash replacement ratio. This result, in conjunction to the chloride concentration profiles discussed above, indicates that in the case of the fly ash-blended specimens, the embedded steel bars lack both physical and chemical protection. The smaller cover to the steel bars, and hence, a high concentration of chloride ions on their surface, coupled with the depletion of calcium hydroxide content in the pore solution, thermodynamically favours anodic dissolution of the iron. The cathodic reaction is also

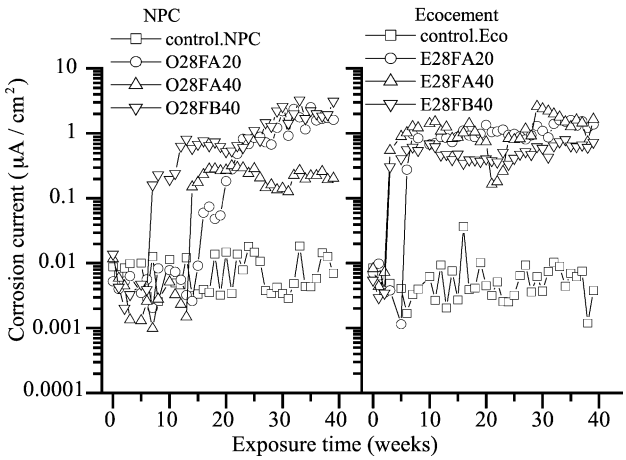

Fig. 8. Corrosion current versus curing time for specimens moist-cured for 28 days before placing in the environmental chamber.

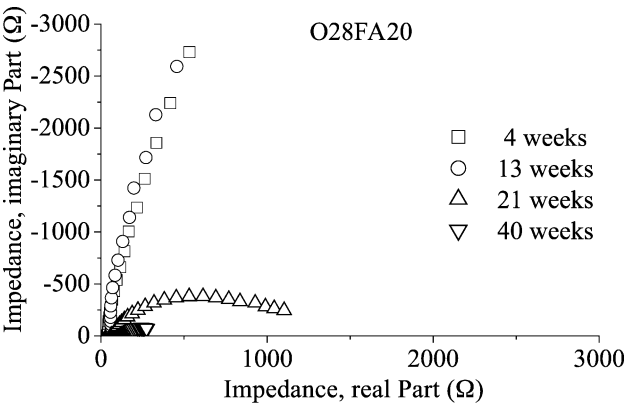

Fig. 10. Impedance plane plots for the NPC specimen with 20% fly ash replacement moist-cured for 28 days before placing in environmental chamber.

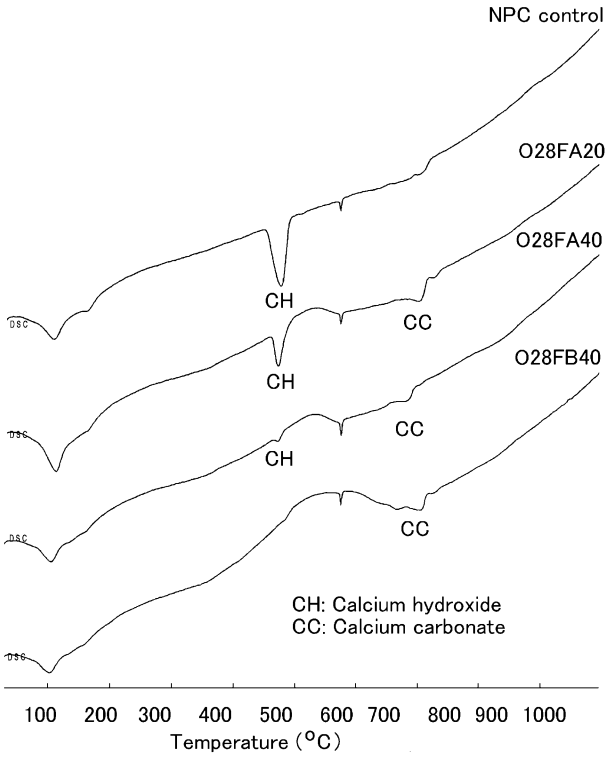

Fig. 11. DSC curves of NPC mortar specimen taken around steel bar.

favoured since at such a shallow cover depth, oxygen supply would also be available, not to mention the cyclic variations in the humidity due to the wetting and drying. It is also seen from the DSC curves that calcium carbonate is

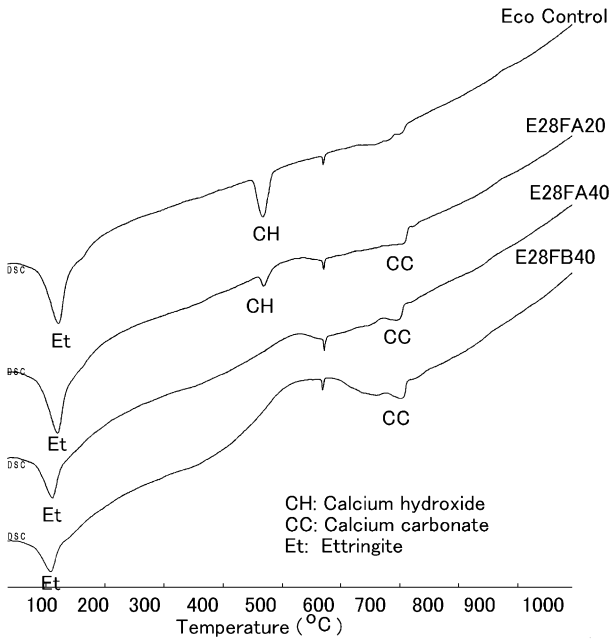

Fig. 12. DSC curves of ecocement mortar specimens taken around steel bar.

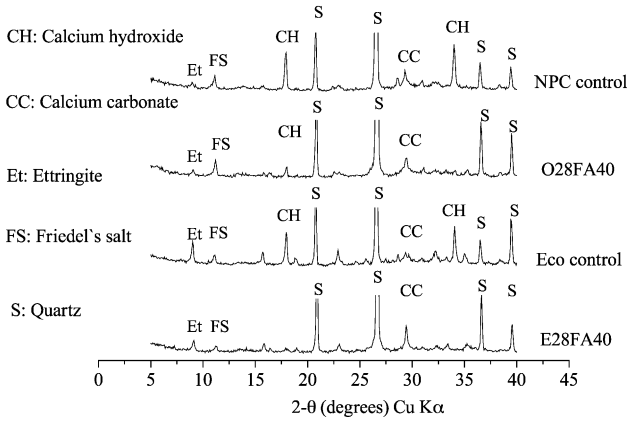

Fig. 13. XRD spectra of ecocement and NPC mortar specimens taken around steel bar.

also present, as evidenced by an endothermic peak at the temperature of around 750 °C. Thus, there is the combined effect of chlorides and carbonation on the corrosive behaviour of the embedded steel bars especially in the fly ash-blended specimens.

Fig. 13 shows the XRD curves of the specimens taken around the steel bars of NPC and ecocement mortar specimens. It is seen that the calcium hydroxide content of the fly ash-blended specimens is lower than that of the control specimens in both NPC and ecocement, indicating the pozzolanic reactivity of the fly ash that consumes calcium hydroxide resulting from hydration of the cement. It is also seen that the calcium hydroxide content of the control specimen of ecocement is less than that of NPC. This suggests that pozzolanic reactivity in the ecocement–fly ash mortars is lower in comparison to that of NPC–fly ash mortars, which agrees with the results of the electrical resistivity measurements. A closer look at the XRD spectra also indicates the formation of ettringite in the ecocement mortars as against that of the NPC mortars. This is because the high sulfate and aluminate content in ecocement favours the formation of Aft phase against Afm phase [7], while that of NPC favours the formation of the Afm phase during hydration.

3.6. Corrosion characteristics

Table 5 shows the weight losses and corroded area obtained from the physical measurements. It is seen that in the case of NPC, the weight losses of the fly ash-blended specimens are larger than that of the control specimen. In the case of ecocement, the amount of corrosion in the control specimen is quite substantial due to the inherent chloride content in the cement itself. The specimen blended with 40% of Fly ash B, however, showed no corrosion.

Fig. 14 also shows a graph of the weight loss obtained from the physical measurements versus that calculated from the values of the corrosion current, using Faraday's law. The

Table 5
Weight loss and corroded area of steel bars measured after corrosion test

7-day precured specimens			28-day precured specimens		
Specimen	Weight loss (%)	Corroded area (%)	Specimen	Weight loss (%)	Corroded area (%)
Control NPC	0.1	5.1	Control NPC	0.0	0.0
O7FA20	0.7	27.3	O287FA20	0.7	33.5
O7FA40	0.4	9.4	O28FA40	0.1	4.1
O7FB40	0.6	22.7	O28FB40	1.2	44.4
Control Eco	0.4	2.8	Control Eco	0.2	5.4
E7FA20	0.9	35.5	E28FA20	0.6	34.4
E7FA40	1.0	44.2	E28FA40	1.2	49.4
E7FB40	0.0	0.0	E28FB40	0.6	35.5

graph shows that the weight loss values obtained from the physical measurements are higher than the corresponding values calculated from the corrosion current, but that there is a good correlation between them. Thus, some form of calibration could be done to convert values obtained from the electrochemical measurements to actual values that would have been obtained from physical measurements. The nondestructive nature of the electrochemical methods makes such an approach more convenient. It should be mentioned that similar measurements performed by the authors using different cement systems also indicated a good correlation between the two values, and in some situations, there was very close agreement to the extent that calibration is not even required.

4. Conclusions

From the results of the various tests performed, the following conclusions could be drawn:

(1) The addition of low-quality fly ashes to both ecocement and NPC results in mortars with lower chloride ingress even though their properties do not meet the requirements of both the JIS A6201-1999 and ASTM C 618 standards.

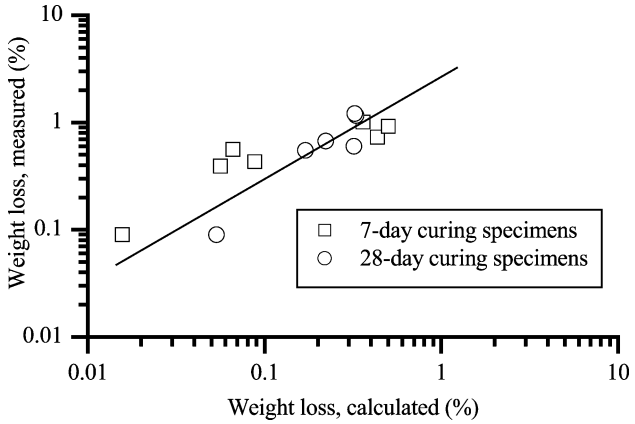

Fig. 14. Weight loss obtained from physical measurement versus values calculated from the corrosion current.

(2) The amount of strength reduction when 20% of both Fly ash A or B is blended with cement is reasonable, and given the reduction in chloride ingress, the fly ash may be used in applications requiring concrete of normal strength without any adverse effect.

(3) Electrical resistivity measurement is an effective nondestructive method for monitoring the pozzolanic reactivity of cement–fly ash systems.

(4) Notwithstanding their poor quality, both Fly ash A and Fly ash B resulted in a significant reduction in the amount of chloride ingress into mortars incorporating them as mineral admixtures.

(5) The addition of both Fly ash A and Fly ash B to the cements resulted in an adverse effect on the corrosive behaviours of the steel bars embedded at shallow cover depths but are expected to provide beneficial effect when the cover depth is increased to 20 mm or more.

Acknowledgments

The authors thank the Eco-Cement Project Team of Taiheiyo Cement for supplying the cement for the experiment and Prof. M. Kawamura, Kanazawa University, for his advice in the experiment.

References

[1] P.K. Mehta, Pozzolanic and cementitious by-products in concrete—Another look, Proceedings of Third CANMENT/ACI Int. Conf., V.M. Malhotra (Ed.), American Concrete Institute, Michigan, ACI SP 114, vol. 1, 1989, pp. 1–43.

[2] P.K. Mehta, Role of pozzolanic and cementitious material in sustainable development of concrete industry, Proceedings of Sixth CANMET/ACI/JCI, Int. Conf. on Fly Ash, Silica Fume and Natural Pozzolans in Concrete, V.M. Malhotra (Ed.), American Concrete Institute, Michigan, ACI SP-178, vol. 1, 1998, pp. 1–20.

[3] K. Torii, T. Sasatani, M. Kawamura, Chloride penetration into concretes incorporating mineral admixtures in marine environment, Proceedings of Sixth CANMET/ACI/JCI, Int. Conf. on Fly Ash, Silica Fume and Natural Pozzolans in Concrete, V.M. Malhotra (Ed.), American Concrete Institute, Michigan, ACI SP-178, vol. 2, 1998, pp. 701–716.

[4] T. Shimoda, Eco-cement: A new Portland cement to solve municipal and industrial waste problems, Proc. of International Congress on Creating with Concrete, Dundee, (1999) 17–30.
[5] K.O. Ampadu, K. Torii, Characterization of ecocement pastes and mortars produced from incinerated ashes, Cem. Concr. Res. 31 (2001) 431–436.
[6] J.P. Broomfield, Assessing corrosion damage on reinforced concrete structures, R.N. Swamy (Ed.), Proc. of Int. Conf. on Corrosion and Corrosion Protection of Steel in Concrete, vol. 1. Sheffield Academic Press, University of Sheffield, Sheffield, 1994, pp. 1–21.
[7] C.D. Lawrence, The constitution and specification of portland cements, in: P.C. Hewlett (Ed.), Lea's Chemistry of Cement and Concrete, fourth ed., Wiley, 1988, pp. 131–188.